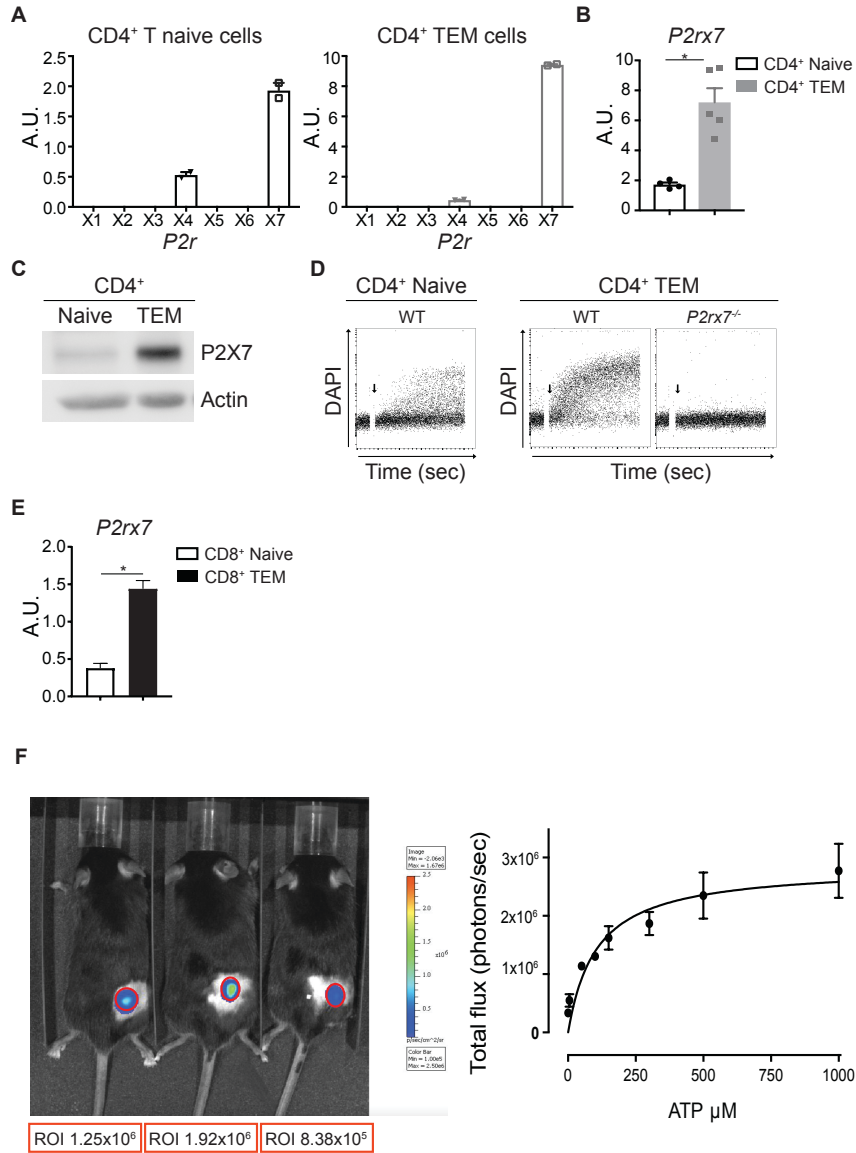
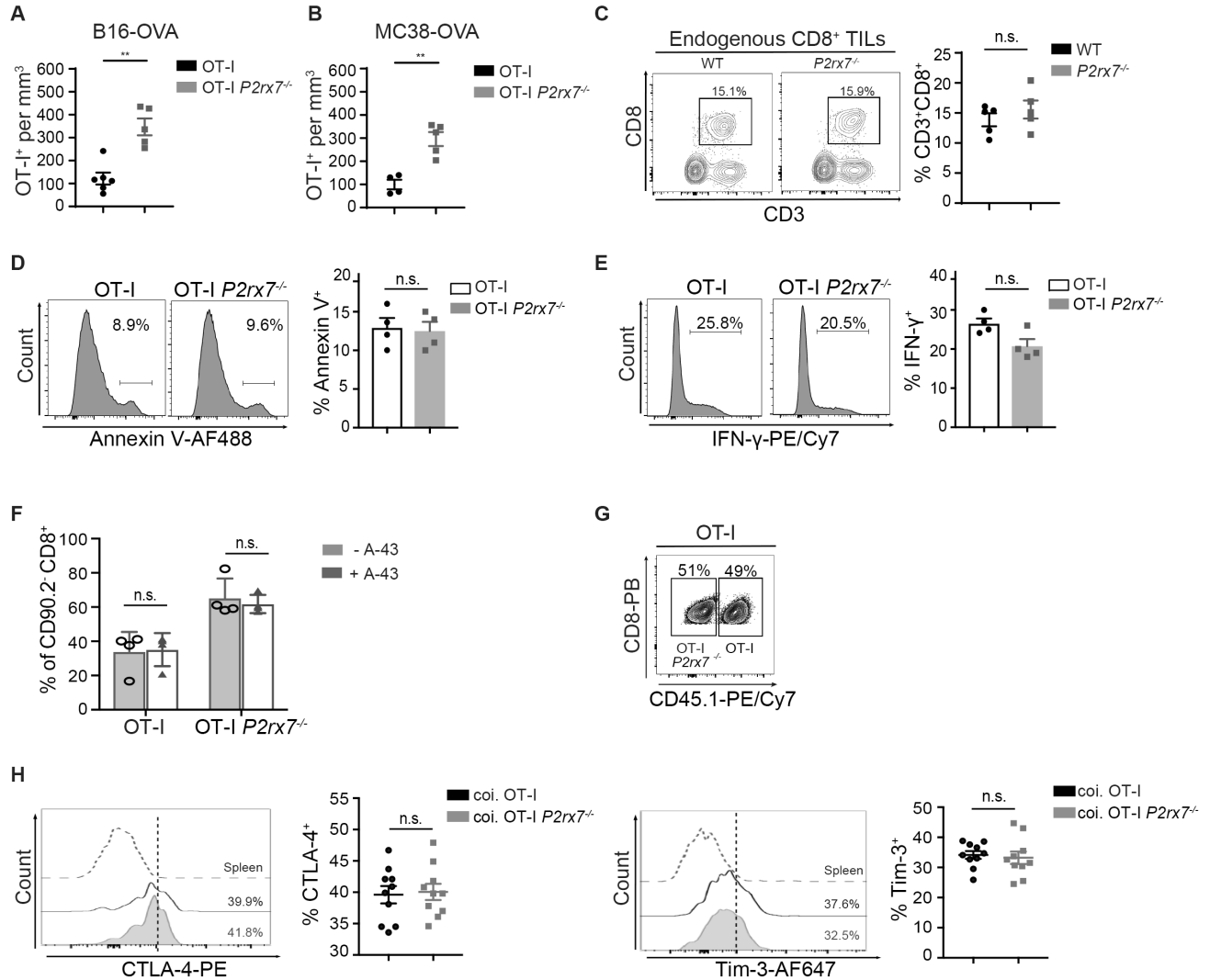


Supplementary figure 1



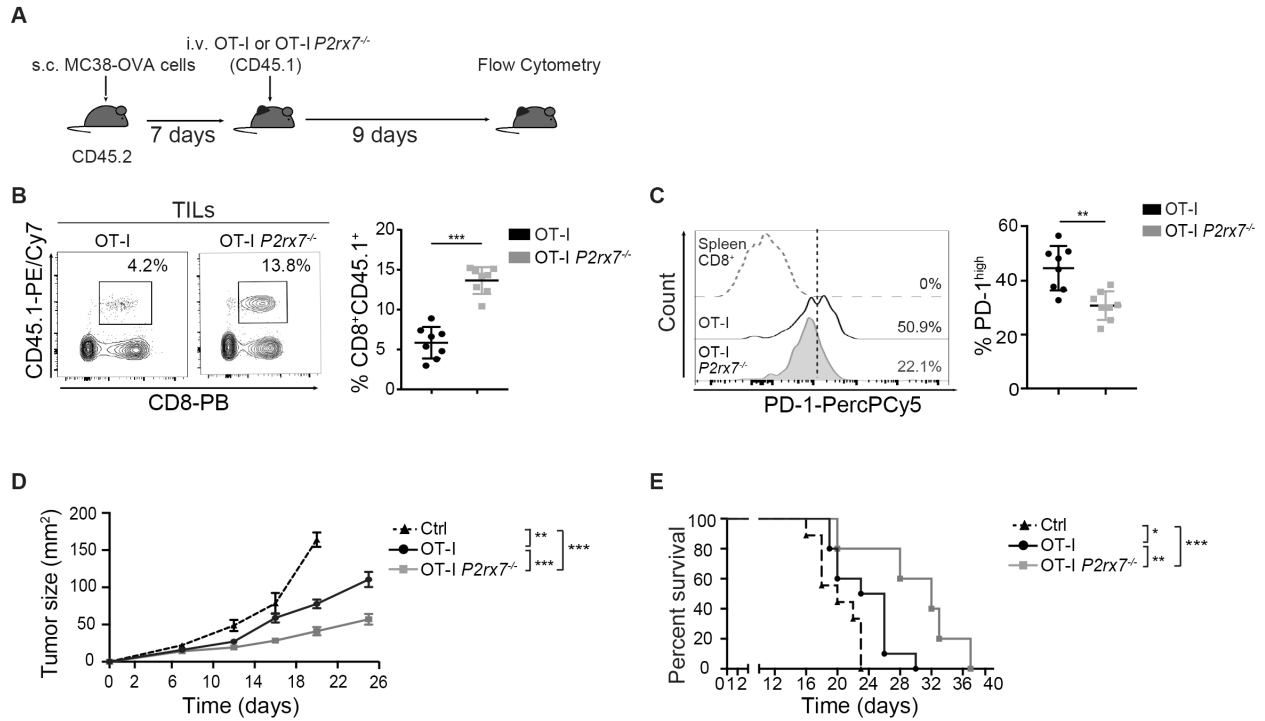
Supplementary Fig. 1. *P2rx7* expression and function in murine T cells and eATP *in vivo* measurement. (A) qRT-PCR of the seven murine *P2rx* genes (X1-X7) in CD4⁺ naïve and TEM cells (mean ± SEM). Data from two experiments with five pooled mice per sample. (B) qRT-PCR of *P2rx7* transcript (mean ± SEM). Data from two experiments with five pooled mice per sample. (C) Quantification of P2X7 protein by western blot. Data from one experiment representative of two (D) Time- monitoring of DAPI permeability in flow cytometry after stimulation with BzATP. *P2rx7*^{-/-} TEM cells were also tested as non-responder control. Data from one experiment representative of three. (E) qRT-PCR of *P2rx7* on sorted CD8⁺ naïve and TEM cells. Data from two independent experiments with six pooled mice per sample. (F) Imaging of C57BL/6 mice with IVIS luminometer at day 7 after engraftment of melanoma B16-pmeLUC cells in the right hip (tumour size $\cong 50 \text{ mm}^2$). Bioluminescence was recorded after i.p. injection of D/luciferin; values (photons/sec) in R.O.I. are reported (left panel). *In vitro* calibration of luminescence with B16F10-pmeLUC cells challenged with increasing concentration of ATP. One min acquisitions at IVIS luminometer are expressed as Total flux (photons/sec) as a function of the added ATP concentration (right panel). A.U., Arbitrary Unit. R.O.I., Region of Interest. Two tailed Mann- Whitney U test. * $p < 0.05$.

Supplementary figure 2



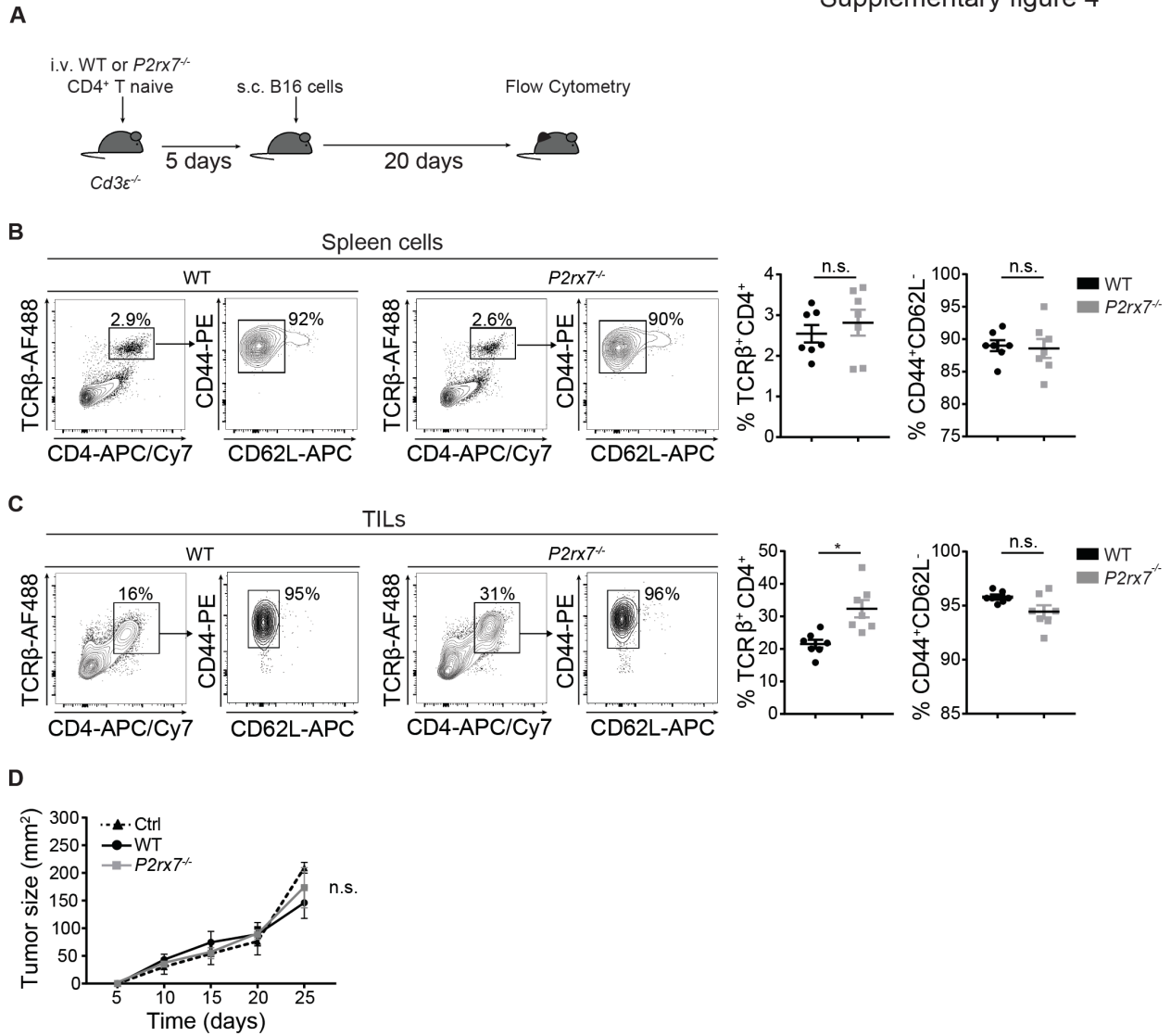
Supplementary Fig.2. Ex vivo recovery of transferred and endogenous CD8⁺ TILs, characterization of OT-I cells before injection and co-transfer, and CTLA-4 and TIM-3 expression in OT-I TILs. (A-B) Statistical analysis (mean ± SEM) of absolute numbers of OT-I cells recovered from B16-OVA (A) and MC38-OVA (B) tumors, adjusted per mm³ of tumor. Data from one experiment representative of two. (C) Representative flow cytometry plots of endogenous TILs, gated as CD3⁺CD8⁺ on CD45.1⁺ cells. One experiment representative of two. (D-E) Flow cytometry histograms and statistical analysis (mean ± SEM) for Annexin-V (D) and IFN-γ secretion (E) in purified *Rag1*^{-/-}/*P2rx7*^{+/-} (OT-I) and *Rag1*^{-/-}/*P2rx7*^{-/-} (OT-I *P2rx7*^{-/-}) cells stimulated with anti-CD3/CD28 antibodies for 72 h (n=4). Data from one experiment representative of two. (F-H) CD45.2/CD90.2 C57BL/6 mice were engrafted with B16-OVA and then co-injected with 1x10⁶ CD45.1⁺CD90.1⁺ *Rag1*^{-/-}/*P2rx7*^{+/-} (OT-I) and 1x10⁶ CD45.2⁺CD90.1⁺ *Rag1*^{-/-}/*P2rx7*^{-/-} (OT-I *P2rx7*^{-/-}) cells. (F) Statistical analysis (mean ± SEM) showing the percentage of OT-I TILs isolated in the presence or absence of the P2X7 inhibitor A-438079 (A-43) 50μM (n=4). Injected cells were selected as CD8⁺CD90.2⁺; OT-I *P2rx7*^{+/-} and OT-I *P2rx7*^{-/-} cells were gated as CD45.1⁺ and CD45.1⁻, respectively. Data from one experiment representative of two. (G) Representative dot plot showing the 1:1 ratio of OT-I *P2rx7*^{+/-} and OT-I *P2rx7*^{-/-} cells prior to co-transfer. (H) Flow cytometry histograms and statistical analysis (mean ± SEM) for CTLA-4 and TIM-3 expression in OT-I TILs. Data from 2 independent experiments. Two-tailed Mann-Whitney U test. n.s. not significant.

Supplementary figure 3



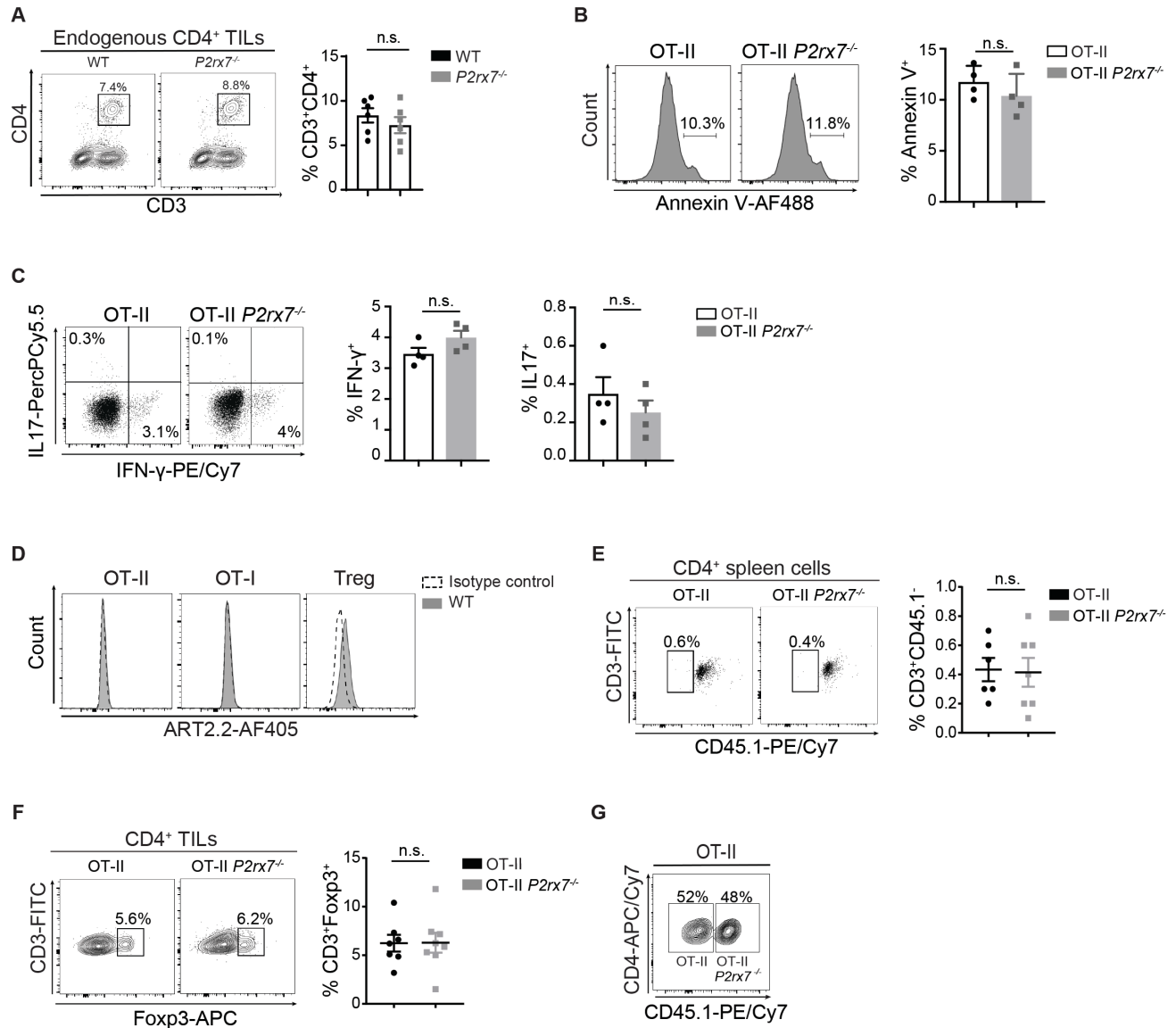
Supplementary Fig.3. Enhanced control of MC38-OVA tumor growth and mice survival by $P2rx7^{-/-}$ OT-I TILs. (A-E) CD45.2⁺ mice were engrafted with MC38-OVA cells and injected with *in vitro* primed 1×10^6 CD45.1⁺CD8⁺ $Rag1^{-/-}/P2rx7^{+/+}$ (OT-I) or $Rag1^{-/-}/P2rx7^{-/-}$ (OT-I $P2rx7^{-/-}$) cells. (A) Experimental design. (B) Representative flow cytometry plots and statistical analysis (mean \pm SEM) for CD45.1⁺CD8⁺ TILs, gated on CD3⁺ cells. (C) Flow cytometry histograms and statistical analysis (mean \pm SEM) for PD-1^{hi} cells within OT-I and OT-I $P2rx7^{-/-}$ TILs, and CD8⁺TCR β ⁺ cells from spleen (Spleen). Percentages of positive cells in each gate are shown. Data from 2 independent experiments (n=8). (D) Kinetics of tumor growth and (E) Kaplan-Meier survival plot. One experiment representative of two, n=9 mice for each group. Two-tailed Mann-Whitney U test for the comparison of two groups or two-way ANOVA for comparison of tumor size was used. Mantel-Cox test for analysis of survival. * p<0.05, ** p<0.01, *** p<0.001, **** p<0.0001

Supplementary figure 4

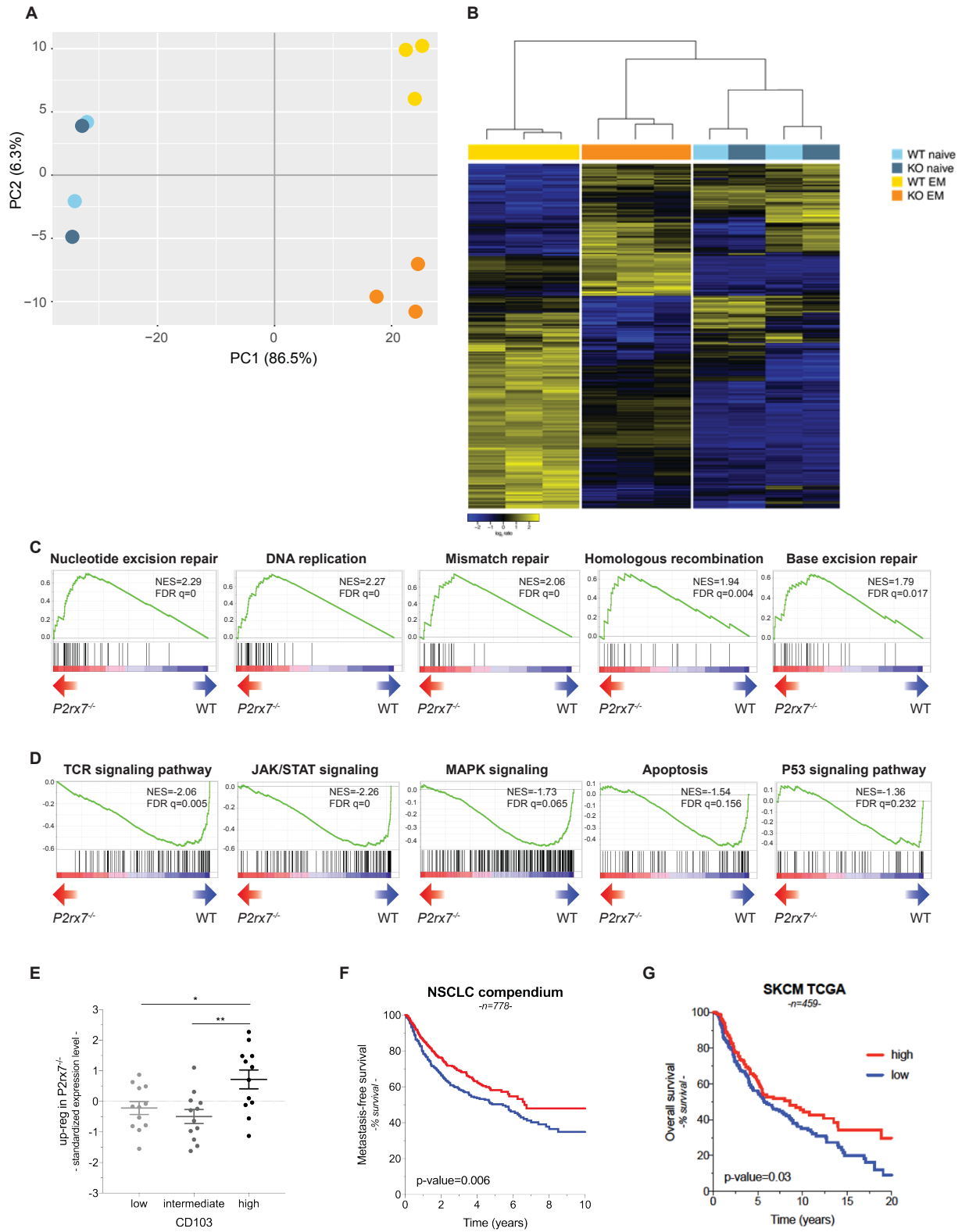


Supplementary Fig. 4. P2X7 activity limits amplification of homeostatically expanded CD4⁺ T naïve cells in B16 melanoma. (A–D) *Cd3ε*^{-/-} mice were adoptively transferred with 2.5×10^5 WT or *P2rx7*^{-/-} CD4⁺ naïve T cells and subsequently engrafted with B16 cells. Data are from a single experiment representative of two. (A) Experimental design. (B) Representative flow cytometry plots and statistical analysis of splenocytes and (C) TILs for percentage of TCRβ⁺CD4⁺ cells among total live cells (see methods for tumors) as well as CD62L⁻CD44⁺ cells on gated CD4⁺TCRβ⁺ cells (mean ± SEM). Percentages of positive cells in each gate are shown. (D) Kinetics of tumor growth. Two-tailed Mann-Whitney U test and two-way ANOVA test were used. n.s. not significant, **p*<0.05.

Supplementary figure 5

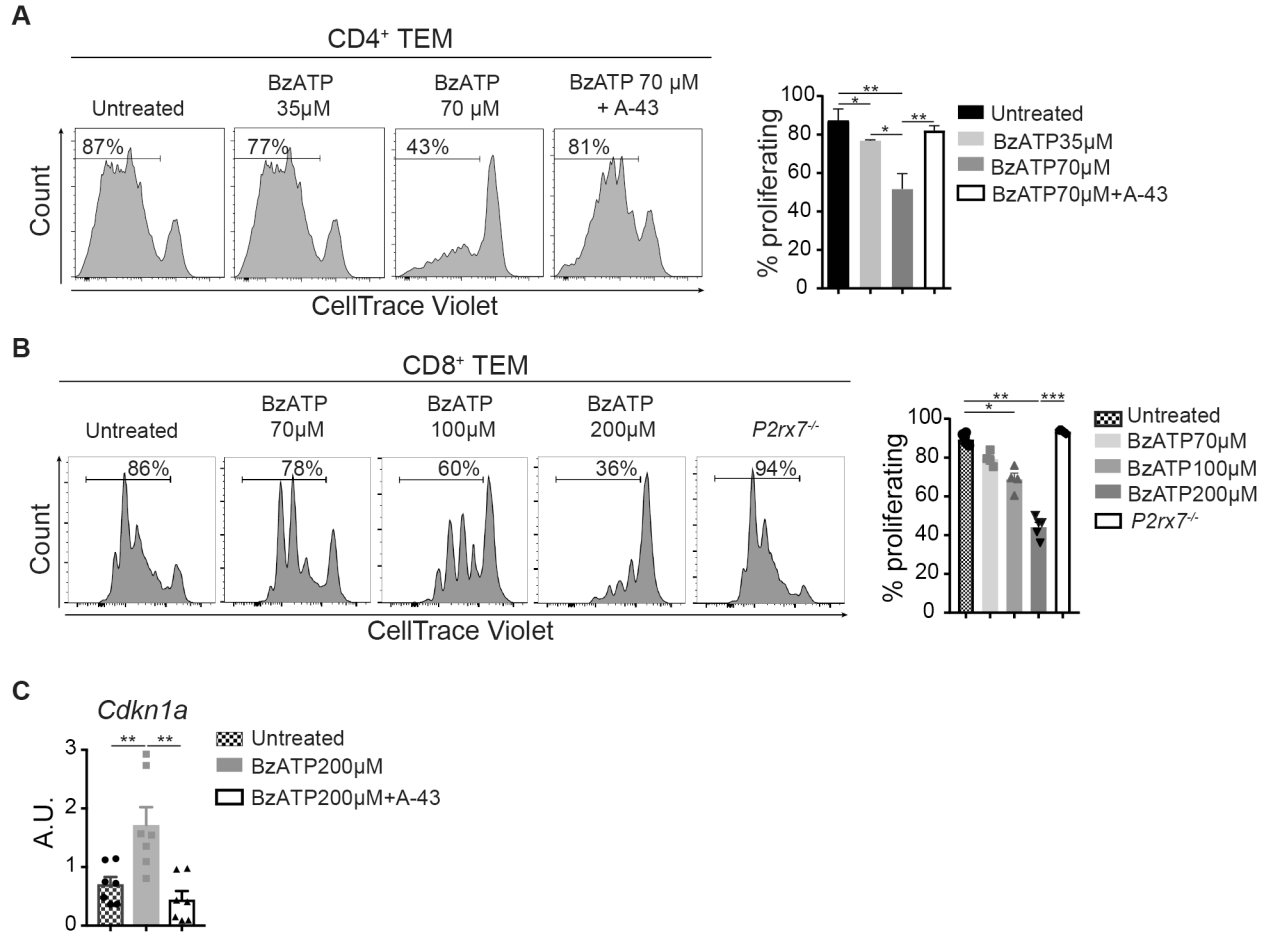


Supplementary figure 6



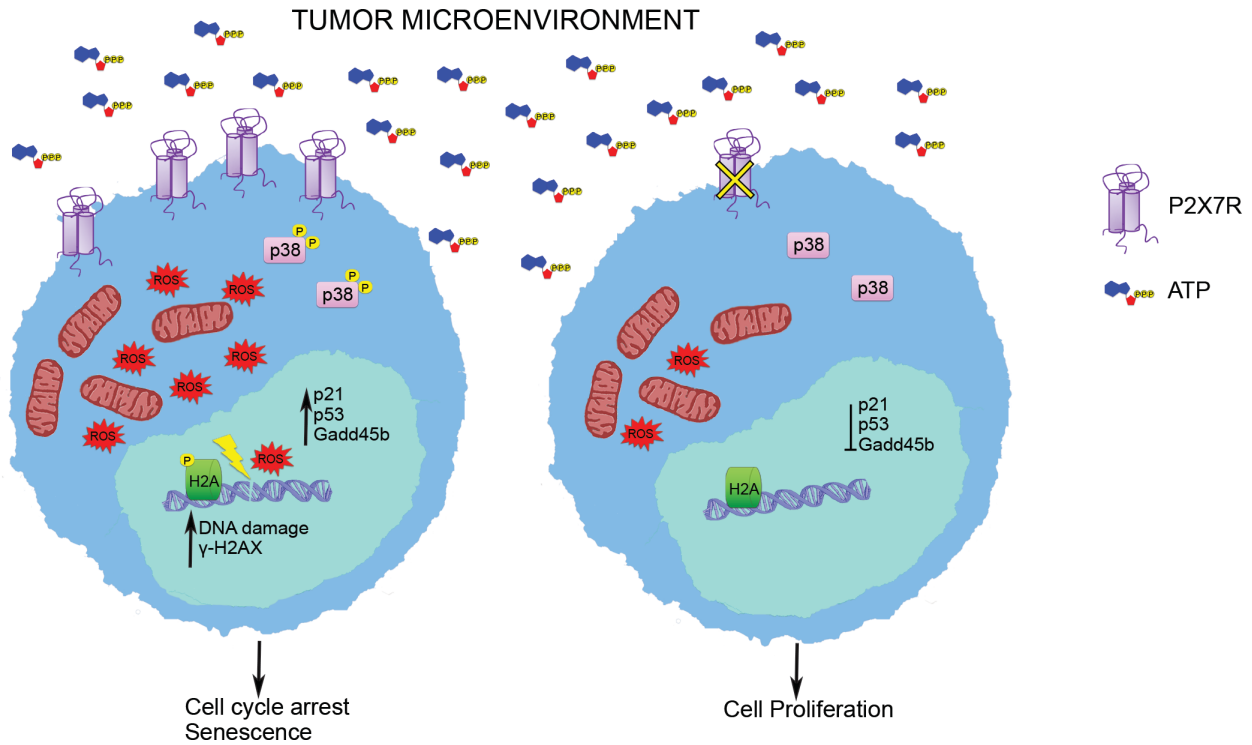
Supplementary Fig.6. Genome-wide expression profiling of *ex vivo* purified CD4⁺ naïve and TEM cells from WT and *P2rx7^{-/-}* mice and enrichment of *P2rx7^{-/-}* over-expressed genes in tumor samples. (A) Unsupervised Principal Component Analysis of gene expression profiles in naïve and TEM cells from *P2rx7^{-/-}* and WT mice using the top 5% of transcripts (904 genes) responsible for the largest variance in the data (see Material and Methods for details). Each dot represents one separated biological sample (WT naïve: *n*=2; *P2rx7^{-/-}* naïve: *n*=2; WT TEM: *n*=3; *P2rx7^{-/-}* TEM: *n*=3). (B) Hierarchical clustering of gene expression profiles in naïve and TEM cells from *P2rx7^{-/-}* and WT mice using the transcriptional signature of 158 upregulated and 255 downregulated genes in *P2rx7^{-/-}* TEM as compared to WT cells (FDR≤5% and absolute fold change≥1.5; see table S1). Each column represents one separated biological sample (WT naïve: *n*=2; *P2rx7^{-/-}* naïve: *n*=2; WT TEM: *n*=3; *P2rx7^{-/-}* TEM: *n*=3). (C) GSEA enrichment plots of gene sets significantly enriched in *P2rx7^{-/-}* TEM cells (*n*=3). (D) Same as in (C) for gene sets significantly enriched in WT TEM cells (*n*=3). (E) Average gene-expression values of genes up-regulated in *P2rx7^{-/-}* TEM cells (FDR≤5% and fold change≥1.5; see table S2) in NSCLC CD8⁺ TILs (*n*=36) stratified according to the status of CD103 (ITGAE) gene (ref. 26). Data are shown as mean ± SEM. Unpaired t-test (* *p*<0.05, ** *p*<0.01) and one-way ANOVA (*p*=0.00468). (F) Kaplan-Meier graphs representing the probability of cumulative metastasis-free survival in lung adenocarcinoma patients (*n*=778) from a compendium of NSCLCs stratified according to the *P2rx7^{-/-}* up-regulation signature. The log-rank test *p* value reflects the significance of the association between *P2rx7^{-/-}* up-regulation signature “high” and longer metastasis-free survival. (G) Same as in (F) for the probability of cumulative overall survival in skin cutaneous melanoma patients (*n*=459) from the TCGA SKCM dataset stratified according to the *P2rx7^{-/-}* upregulation signature. The log-rank test *p* value reflects the significance of the association between *P2rx7^{-/-}* up-regulation signature “high” and longer overall survival.

Supplementary figure 7



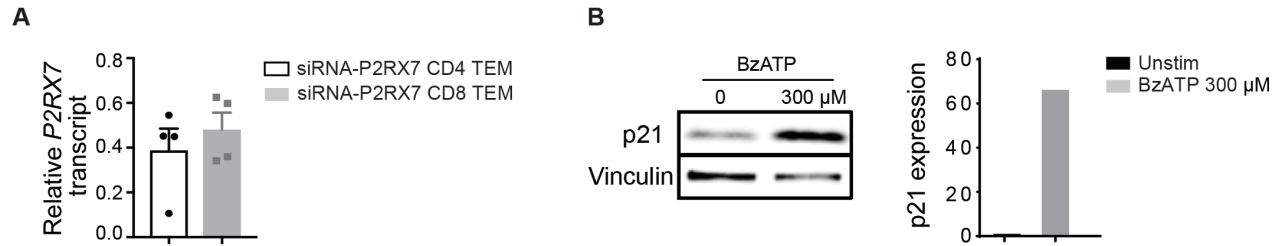
Supplementary Fig. 7. P2X7 mediated inhibition of TEM cell proliferation and induction of *Cdkn1a* in CD8⁺ TEM cells. (A-C) Representative histograms of CellTrace Violet dilution and statistical analysis of proliferating cells (mean \pm SD). Numbers in the histogram plots represent the percentage of proliferating cells. (A) WT CD4⁺ TEM cells were stimulated with anti-CD3/CD28 antibodies for 72 h in the presence of the indicated concentrations of BzATP and A-438079 (A-43) 50µM. Data are from three independent experiments with five pooled mice per sample. (B) Mouse WT and *P2rx7*^{-/-} CD8⁺ TEM cells were stimulated as above in the presence of the indicated concentrations of BzATP (mean \pm SD). Data from two independent experiments (n=5). (C) qRT-PCR of *Cdkn1a* performed on CD8 WT TEM cells either untreated, treated with BzATP 200 µM or pretreated with A- 438079 50 µM (mean \pm SEM, n=7) Data are from two independent experiments. Two-tailed Mann-Whitney U test for the comparison of two groups or Kruskal-Wallis test for the comparison of more than two groups. * p<0.05, ** p<0.01 *** p<0.001.

Supplementary figure 8



Supplementary Fig.8. Model of P2X7 signaling in TILs. Stimulation of P2X7 receptor in TILs by eATP present in the TME promotes p38 MAPK phosphorylation and mitochondrial ROS generation. DNA damage and phosphorylation of H2A.X histone (γ H2A.X) result in cell cycle arrest by activation of the p53/p21 pathway that leads to cellular senescence. Lack of P2X7 activity in TILs results in protracted cell proliferation, resistance to senescence and enhanced tumoricidal function.

Supplementary figure 9



Supplementary Fig.9. Knock-down of *P2RX7* by siRNA and western blot for p21^{Waf1/Cip1} in human TEM cells. (A) qRT-PCR for *P2RX7* transcripts in sorted human CD4⁺ (left) and CD8⁺ (right) TEM cells transfected with *P2RX7* siRNA (siRNA-*P2RX7*). Values were normalized to *P2RX7* transcripts detected in cells transfected with a control siRNA (mean \pm SEM, n=4). Data are from one experiment representative of two. (B) Western blot on protein extracts from human TEM cells either untreated or stimulated with BzATP 300 μ M for 24 h. Densitometric values of p21^{Waf1/Cip1} were normalized with Vinculin. Data are from one experiment representative of two.